

# Cyclotron Resonance of Composite Fermions

I. V. Kukushkin,<sup>1,2</sup> J. H. Smet,<sup>1</sup> K. von Klitzing,<sup>1</sup> and W. Wegscheider<sup>3,4</sup>

Received February 4, 2003

The introduction of suitable fictitious entities occasionally permits to cast otherwise difficult strongly interacting many-body systems in a single particle form. We can then take the customary physical approach, using concepts and representations which formerly could only be applied to systems with weak interactions, and yet still capture the essential physics. A most notable recent example occurs in the conduction properties of a two-dimensional electron system (2DES), when exposed to a strong perpendicular magnetic field  $B$ . They are governed by electron–electron interactions, that bring about the fractional quantum hall effect (FQHE). S. Das Sarma and A. Pinczuk (eds.), *Perspectives on Quantum Hall Effects* (Wiley, New York, 1996). Composite fermions, that do not experience the external magnetic field but a drastically reduced effective magnetic field  $B^*$ , were identified as apposite quasi-particles that simplify our understanding of the FQHE. J. K. Jain, *Phys. Today*, 39–45 (2000). J. K. Jain, *Phys. Rev. Lett.* **63**, 199–202 (1989). They precess, like electrons, along circular cyclotron orbits, with a diameter determined by  $B^*$  rather than  $B$ . B. I. Halperin, P. A. Lee, and N. Read, *Phys. Rev. B* **47**, 7312–7343 (1993). O. Heinonen, (ed.), *Composite Fermions* (World Scientific, Singapore, 1998). R. R. Du, H. L. Stormer, D. C. Tsui, L. N. Pfeiffer, and K. W. West, *Phys. Rev. Lett.* **70**, 2944–2947 (1993). R. R. Du *et al.*, *Phys. Rev. Lett.* **75**, 3926–3929 (1995). R. L. Willett, R. R. Ruel, K. W. West, and L. N. Pfeiffer, *Phys. Rev. Lett.* **71**, 3846–3849 (1993). V. J. Goldman, B. Su, and J. K. Jain, *Phys. Rev. Lett.* **72**, 2065–2068 (1994). J. H. Smet, D. Weiss, R. H. Blick, G. Lütjering, and K. von Klitzing, *Phys. Rev. Lett.* **77**, 2272–2275 (1996). The frequency of their cyclotron motion remained hitherto enigmatic, since the effective mass is no longer related to the band mass of the original electrons and is entirely generated from electron–electron interactions. Here, we demonstrate the enhanced absorption of a microwave field that resonates with the frequency of their circular motion. From this cyclotron resonance, we derive a composite fermion effective mass that varies from 0.7 to 1.2 times the electron mass in vacuum as their density is tuned from  $0.6 \times 10^{11}/\text{cm}^2$  to  $1.2 \times 10^{11}/\text{cm}^2$ .

**KEY WORDS:** cyclotron; composite fermions; surface acoustic waves.

Composite Fermions (CFs) are electrons dressed with two flux quanta (more generally an even number), that point opposite to the external  $B$ -field [1–3]. This attachment is a natural way to minimize the energy of the 2DES, since the associated vortex expels

other electrons from its neighborhood and decreases the repulsive interaction between the 2D-electrons. If two flux quanta penetrate the sample per electron, i.e. if the filling factor  $\nu$  equals 1/2, the external field is effectively compensated, and a metallic state of these compound particles emerges [3]. This state can be characterized by a Fermi wavevector and energy. A deviation from exact half filling results in the appearance of a nonzero effective field  $B^*$ , that quantizes the CF-motion and discretizes their energy spectrum into Landau levels. In this framework, the FQHE [4] is a manifestation of this Landau quantization and is equivalent to the integer quantum Hall effect of

<sup>1</sup>Max-Planck-Institut für Festkörperforschung, D-70569 Stuttgart, Germany.

<sup>2</sup>Institute of Solid State Physics, RAS, 142432, Chernogolovka, Russia.

<sup>3</sup>Walter Schottky Institut, Technische Universität München, D-85748 Garching, Germany.

<sup>4</sup>Institut für Experimentelle und Angewandte Physik, Universität Regensburg, D-93040 Regensburg, Germany.

CFs. A variety of experimental observations [5–10] can be understood in semiclassical terms of nearly independent CFs.

Since the kinetic energy of electrons is entirely quenched in the course of applying a  $B$ -field, the CF cyclotron mass is not a renormalized version of the electron conduction band mass, but must be generated entirely from electron–electron interactions [4]. The search of the CF cyclotron resonance requires substantial sophistication over conventional methods used to detect the electron cyclotron resonance, since Kohn’s theorem [11] must be outwitted. It states that in a translationally invariant system radiation can only couple to the center-of-mass coordinate and can not excite other internal degrees of freedom. Phenomena originating from electron–electron interactions will thus not be reflected in the absorption spectrum. An elegant way to bypass this theorem is to impose a periodic density modulation to break translational invariance. The nonzero wavevectors defined by the appropriately chosen modulation may then offer access to the cyclotron transitions of CFs, even though they are likely to remain very weak. Therefore, the development of an optical detection scheme, that boosts the sensitivity to resonant microwave absorption by up to two orders of magnitude in comparison with traditional techniques, was a prerequisite for our studies. Furthermore, we exploited to our benefit the accidental discovery that microwaves, already incident on the sample, set up a periodic modulation through the excitation of surface acoustic waves (SAW).

The 2DES, patterned into a disk with 1-mm diameter [12], is placed near the end of a 16- or 8-mm short-circuited waveguide in the electric field maximum of the microwave excitation inside a  $\text{He}^3$ -cryostat. At a fixed  $B$ -field, luminescence spectra *with* and *without* microwave excitation were recorded consecutively. The differential luminescence spectrum is obtained when subtracting both these spectra. To improve signal-to-noise ratio, the same procedure was repeated  $N$  times ( $N = 2\text{--}20$ ). Subsequently, we integrated the absolute value of the averaged differential spectrum over the entire spectral range and hereafter refer to the value of this integral as *the microwave absorption amplitude*. The same procedure is then repeated for different values of  $B$ . To establish trustworthiness in this unconventional scheme, we apply it in Fig. 1 to the well-known case of the electron–cyclotron resonance  $\omega_{\text{cr}} = eB/m^*$ , with  $m^*$  the effective mass of GaAs ( $0.067 m_0$ ). Due to its limited size, the sample also supports a dimensional plasma mode with a frequency  $\omega_{\text{p}}$ , that depends on

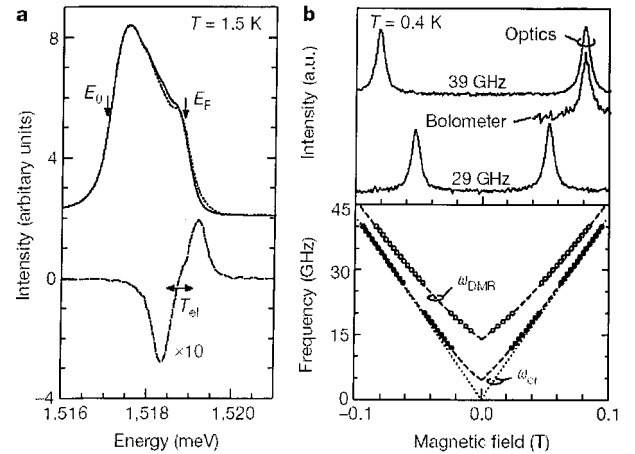
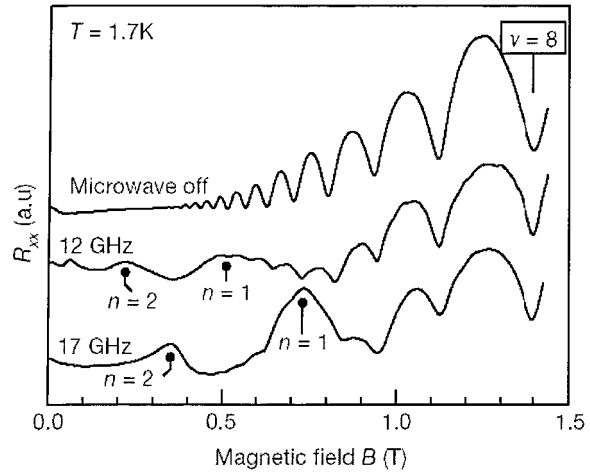


**Fig. 1.** Illustration of the optical scheme to detect resonant microwave absorption for the electron cyclotron-magnetoplasmon hybrid mode at low  $B$ -fields. GaAs/ $\text{Al}_{0.3}\text{Ga}_{0.7}\text{As}$  heterostructures, containing a single 30-nm wide quantum well, served the investigation. The embedded 2DESs have densities and electron transport mobilities between  $0.6\text{--}1.5 \times 10^{11}/\text{cm}^2$  and  $3\text{--}5 \times 10^6 \text{ cm}^2/\text{Vs}$  respectively. (a) Luminescence spectrum in the presence of (dotted line) and without (solid line) a  $50 \mu\text{W}$  microwave excitation of 18 GHz obtained on a disk-shaped 2DES with a diameter of 1 mm and carrier density  $n_s = 5.8 \times 10^{10}/\text{cm}^2$  at a magnetic field  $B = 22 \text{ mT}$ . The spectra were recorded by using a CCD-camera, a double-grating spectrometer that provides a spectral resolution of  $0.03 \text{ meV}$ , and a stabilized semiconductor laser operating at a wavelength of  $750 \text{ nm}$  and approximately  $100 \mu\text{W}$  of cw-power. In the vicinity of the Fermi energy  $E_F$  the spectrum is affected significantly under resonant microwave excitation due to heating. The dashed line represents the differential luminescence spectrum. The width of the differential spectrum reflects the increased electron temperature  $T_c$ . The integration of its absolute value across the entire spectral range yields the microwave absorption amplitude. (b) Top panel: The microwave absorption amplitude at 29 GHz and 39 GHz as a function of  $B$ -field by recording differential luminescence spectra as in (a) for 1 mT field increments at  $n_s = 1.09 \times 10^{11}/\text{cm}^2$ . The peaks, symmetrically arranged around zero field, are identified as the dimensional magnetoplasma-cyclotron hybrid mode. The inset shows a conventional bolometer measurement. Bottom panel: resonance position for  $n_s = 1.09 \times 10^{11}$  (open circles) and  $1.1 \times 10^{11}/\text{cm}^2$  (solid circles) as a function of incident microwave frequency. The intervals 10–20 GHz and 27–40 GHz were covered. The dashed lines represent the theoretical dependence of the hybrid dimensional magnetoplasma-cyclotron resonance. The dotted line corresponds to the cyclotron mode only.

both the density  $n_{2D}$  and diameter  $d$  of the sample, according to  $\omega_{\text{p}}^2 = 3\pi^2 n_{2D} e^2 / (2m^* \epsilon_{\text{eff}} d)$ . The plasma and cyclotron mode hybridize and the resulting resonance frequency of the upper dimensional magnetoplasma-cyclotron mode  $\omega_{\text{DMR}}$  equals  $\omega_{\text{cr}}/2 + [\omega_{\text{p}}^2 + (\omega_{\text{cr}}/2)^2]^{1/2}$  [12,13]. The optical method indeed recovers this mode. A comparison with the theoretical expression for  $\omega_{\text{DMR}}$  yields excellent agreement. No fitting is required, since the density can

be independently extracted from the luminescence at higher  $B$ -fields, where Landau levels can be resolved. At sufficiently low density, the influence of  $\omega_p$  on the hybrid mode drops and one recovers at large enough  $B$  the anticipated  $\omega_{cr} = eB/m^*$ -dependence. Further details of the electron cyclotron resonance are discussed elsewhere [12]. Additional support for the validity of the detection method comes from a comparison with measurements based on the conventional approach using a bolometer (inset Fig. 1b). Not only does one find the same resonance position, but also the same line shape. The only difference is the improved signal-to-noise ratio (30–100 times) for the optical detection scheme, that enables to observe the electron cyclotron resonance at microwave levels below 10 nW.

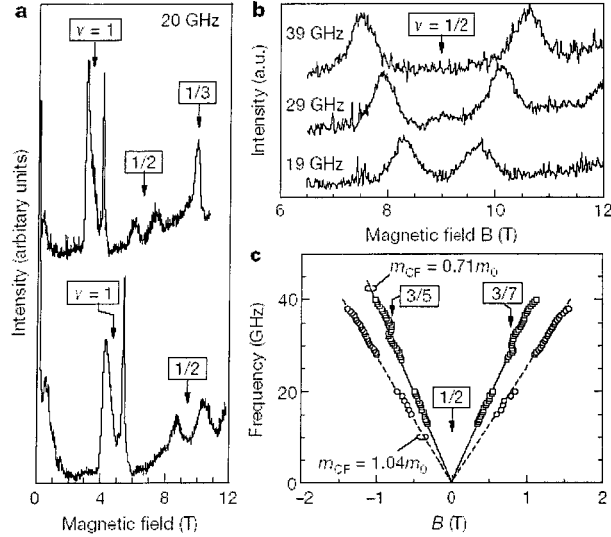
Disorder and the finite dimensions of the sample in principle suffice to break translational invariance as attested by the interaction of the cyclotron and dimensional plasma mode. However, they provide access to internal degrees of freedom other than the center-of-mass motion of the electrons either at poorly defined wavevectors or too small a wavevector for appropriate sample sizes. Therefore, the imposition of an additional periodic density modulation, that introduces larger and well-defined wavevectors to circumvent Kohn's theorem, is desirable. Transport experiments in the hall bar geometry disclosed that additional processing is not required, since the microwaves, already incident on the sample, concomitantly induces a periodic modulation at sufficiently high power. A clear signature is the appearance of commensurability oscillations in the magnetoresistance due to the interplay between the  $B$ -dependent cyclotron radius of electrons and the length scale imposed by the modulation [14]. Examples are displayed in Fig. 2 and resemble the data in [15], where the modulation is produced with the help of SAW-transducers. Here, the following scenario is conceivable. Owing to the piezoelectric properties of the  $\text{Al}_x\text{Ga}_{1-x}\text{As}$ -crystal, the radiation is partly transformed into SAW with opposite momentum, so that both energy and momentum are conserved. Reflection from cleaved boundaries of the sample then produces a standing wave with a periodicity determined by the sound wavelength. Photoexcitation creates a very poorly conducting parallel 3D-layer in the Si-doped portion of the  $\text{AlGaAs}$ -barrier and may enhance the influence of the standing acoustic waves. Carriers are collected in the nodes and affect the local density of the 2DES. The involvement of sound waves can be deduced from transport data, since from the minima we expect the modulation pe-



**Fig. 2.** Magnetotransport data without (top curve) and under  $100 \mu\text{W}$  of microwave radiation at 12 (middle curve) and 17 GHz (bottom curve). Curves are offset for clarity. Besides the well-known Shubnikov-de Haas oscillations, additional magnetoresistance oscillations appear under microwave radiation. They are commonly observed in 2DESs on which a static periodic modulation of the density has been imposed. There is no sign of such commensurability effects in the corresponding optical experiments. This can ultimately be traced back to the fact that, contrary to optical quantities, transport is also sensitive to semiclassical phenomena unrelated to changes in the density of states.

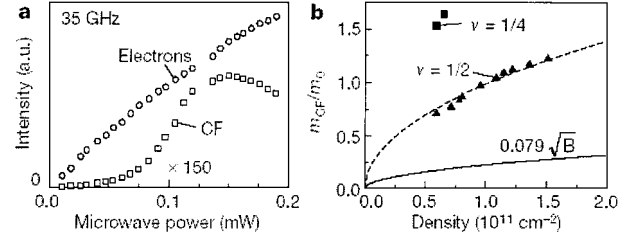
riod to be approximately 200 and 250 nm for frequencies of 17 and 12 GHz respectively. The ratio of this period to the sound wavelength at these frequencies is 1.12 and 1.15.

Fig. 3a depicts the  $\mu\text{W}$ -absorption amplitude up to high  $B$ -fields. A part from the strong dimensional magnetoplasma-cyclotron resonance signal at low  $B$ -field discussed above, several peaks, that scale with a variation of the density, emerge near filling 1, 1/2 and 1/3. Those peak positions associated with  $\nu = 1$  and 1/3 remain fixed when tuning the microwave frequency and are ascribed to heating induced by non-resonant absorption of microwave power. In contrast, the weak maxima surrounding filling 1/2 readily respond to a change in frequency as illustrated in Fig. 3b. They are symmetrically arranged around half filling and their splitting grows with frequency. The  $B$ -dependence is summarized in Fig. 3c for two densities. To underline the symmetry,  $B^*$  was chosen as the abscissa. The linear relationship between frequency and field extrapolates to zero at vanishing  $B^*$ . We do not expect a deviation at small  $B^*$  due to a plasma-like contribution as in Fig. 1c. Excitations for the 1/3, 2/5, 3/7 and other fractional quantum Hall states exhibit in numerical simulations no magnetoplasmon-like linear contribution to the dispersion at small values



**Fig. 3.** Microwave absorption amplitude and peak position for high  $B$ -fields in the samples with a disk shaped mesa at  $T = 0.4$  K. (a) Microwave absorption amplitude at high magnetic fields for  $n_s = 0.81 \times 10^{11}$  and  $1.15 \times 10^{11}/\text{cm}^2$  and frequency of 20 GHz. The response near  $\nu = 1$  and  $1/3$  does not shift with frequency. (b) Microwave absorption amplitude in the vicinity of  $\nu = 1/2$  (20 mT step size) at three different frequencies and  $n_s = 1.09 \times 10^{11}/\text{cm}^2$ . The peak values are nearly two orders of magnitude weaker and considerably wider (about 30–50 times) than those due to the electron cyclotron resonance. (c) Position of the CF cyclotron mode as a function of the effective magnetic field  $B^*$  for  $n_s = 1.09 \times 10^{11}/\text{cm}^2$  (circles) and  $n_s = 0.59 \times 10^{11}/\text{cm}^2$  (squares). The CF effective mass equals  $1.04 m_0$  and  $0.71 m_0$  respectively. The resonances remain visible even if the 2DES condenses in the gapfull fractional quantum Hall states at filling factors  $3/5$  and  $3/7$ .

of  $k$  [16]. We conclude that the resonance in Fig. 3 is the long searched for cyclotron resonance of CFs. Geometric resonances (GR), as they occur in transport at low fields due to the density modulation (Fig. 2), are excluded as an alternative interpretation for the observed features on the following grounds: I. In the optical data, only the electron cyclotron resonance peak is observed. Contrary to optical quantities, transport is also sensitive to semiclassical phenomena unrelated to changes in the density of states. II. Even if the 2DES condenses in a FQHE-state and the chemical potential is located in a gap, the resonance peaks surrounding  $\nu = 1/2$  occur (Fig. 3c). Commensurability effects are not observable in this regime. III. The observation of GRs requires that the density modulation is temporally static on the time scale with which CFs execute their cyclotron orbit. For electrons at low fields this condition is met and accordingly transport displays GRs. For the anticipated enhanced mass of CFs, this condition is violated. IV. Analogous reso-



**Fig. 4.** Cyclotron resonance amplitude as a function of incident microwave power and cyclotron mass of CFs at  $\nu = 1/2$  and  $1/4$  for various carrier densities. (a) Incident microwave power dependence of the amplitude at the cyclotron resonance (circles for electrons, squares for CFs). (b) Dependence of the CF effective mass near  $\nu = 1/2$  on the carrier density  $n_s$  (solid triangles). The mass for  $\nu < 1/2$  is systematically a few percent heavier than for  $\nu > 1/2$ . The dashed line is a square-root-fit to the data. The solid curve is the prediction from theory reported in [17]. Analogous resonance peaks have also been detected around  $\nu = 1/4$ . The corresponding effective mass values are indicated as solid squares for two different densities. The large discrepancy in the extracted values of the effective masses for  $\nu = 1/2$  and  $\nu = 1/4$  allows to exclude that the resonant microwave absorption peaks originate from a commensurability effect.

nance peaks were also detected for the higher order CFs around  $\nu = 1/4$ . Since this CF metallic state is characterized by the same Fermi wavevector, GRs would show up at the same distance from  $\nu = 1/4$  as they do at  $\nu = 1/2$ . The observed peaks are located at different positions rendering a commensurability picture untenable (see below Fig. 4b).

In contrast to electron–cyclotron resonance, the intensity of the CF cyclotron resonance is a strong nonlinear function of  $\mu\text{W}$ -power (Fig. 4a). Moreover, its observability only at high power correlates with the first appearance of commensurability oscillations. The drop in intensity at even higher power is most probably due to heating. The intensity diminishes to zero at temperatures above 0.7 K, whereas the electron–cyclotron resonance persists up to  $T > 2$  K. The slope of the CF cyclotron frequency as a function of  $B^*$  in Fig. 3c defines the cyclotron mass  $m_{\text{cr}}^{\text{cf}}$ . This mass is set by the electron–electron interaction scale, so that a square-root behavior on density or  $B$ -field is forecasted from a straightforward dimensional analysis [4]. Numerical calculations predict  $m_{\text{cr}}^{\text{cf}}/m_0 = 0.079 (B[T])^{1/2}$  for an ideal 2DES, not including Landau level mixing or finite width contributions [17]. The data, shown in Fig. 4b, confirm qualitatively the strong enhancement in comparison with the electron mass (more than 10 times), however a fit to the square-root dependence requires a prefactor that is four times larger. Previously reported mass values based on activation energy gap

measurements [18,19] must be distinguished from the cyclotron mass. The former corresponds to the limit of infinite momentum, whereas here  $k$  approaches zero. Moreover, activation gaps can only be extracted at well-developed fractional quantum hall states and their accurate determination suffers from disorder-induced broadening. These and other limitations have been discussed in [19], for example. The technique discussed here can be performed at arbitrary filling factors.

In summary, the fortuitous breaking of translational invariance induced by the microwave irradiation combined with the virtues of an optical detection scheme for resonant absorption has enabled to unveil the cyclotron resonance frequency of CFs and to measure the corresponding cyclotron mass.

#### ACKNOWLEDGMENTS

Partial support by the Volkswagen Stiftung, the Russian Fund of Fundamental Research, INTAS, the German Ministry of Science and Education, and the German Physical Society is gratefully acknowledged.

#### REFERENCES

1. J. K. Jain, *Phys. Today*, 39–45 (2000).
2. J. K. Jain, *Phys. Rev. Lett.* **63**, 199–202 (1989).
3. B. I. Halperin, P. A. Lee, and N. Read, *Phys. Rev. B* **47**, 7312–7343 (1993).
4. S. Das Sarma and A. Pinczuk (eds.), *Perspectives on Quantum Hall Effects* (Wiley, New York, 1996).
5. O. Heinonen, (ed.), *Composite Fermions* (World Scientific, Singapore, 1998).
6. R. R. Du, H. L. Stormer, D. C. Tsui, L. N. Pfeiffer, and K. W. West, *Phys. Rev. Lett.* **70**, 2944–2947 (1993).
7. R. R. Du *et al.*, *Phys. Rev. Lett.* **75**, 3926–3929 (1995).
8. R. L. Willett, R. R. Ruel, K. W. West, and L. N. Pfeiffer, *Phys. Rev. Lett.* **71**, 3846–3849 (1993).
9. V. J. Goldman, B. Su, and J. K. Jain, *Phys. Rev. Lett.* **72**, 2065–2068 (1994).
10. J. H. Smet, D. Weiss, R. H. Blick, G. Lütjering, and K. von Klitzing, *Phys. Rev. Lett.* **77**, 2272–2275 (1996).
11. W. Kohn, *Phys. Rev.* **123**, 1242–1244 (1961).
12. S. I. Gubarev *et al.*, *JETP Lett.* **72**, 324–328 (2000).
13. S. J. Allen, H. L. Stormer, and J. C. M. Hwang, *Phys. Rev. B* **28**, 4875–4877 (1983).
14. R. R. Gerhardts, D. Weiss, and K. von Klitzing, *Phys. Rev. Lett.* **62**, 1173–1176 (1989).
15. J. M. Shilton *et al.*, *Phys. Rev. B* **51**, 14770–14773 (1995).
16. J. K. Jain and R. K. Kamilla, in *Composite Fermions*, O. Heinonen, ed. (World Scientific, Singapore, 1998), pp. 1–80.
17. K. Park and J. K. Jain, *Phys. Rev. Lett.* **80**, 4237–4240 (1998).
18. R. R. Du, H. L. Stormer, D. C. Tsui, L. N. Pfeiffer, and K. W. West, *Phys. Rev. Lett.* **70**, 2944–2947 (1993).
19. R. L. Willett, in *Composite Fermions*, O. Heinonen, ed. (World Scientific, Singapore, 1998), pp. 349–431.